Supplement

On the semidiurnal variation in surface rainfall rate over the tropics in a global cloud-resolving model simulation and satellite observations

Toshiro INOUE[1]
Atmosphere and Ocean Research Institute, The University of Tokyo, Kashiwa, Chiba, Japan

Kavirajan RAJENDRAN
Multi-Scale Modelling Programme, CSIR Fourth Paradigm Institute, Bangalore, India

Masaki SATOH
Atmosphere and Ocean Research Institute, The University of Tokyo, Kashiwa, Chiba, Japan

Hiroaki MIURA
Department of Earth and Planetary Science, The University of Tokyo, Tokyo, Japan

S. 1 Eastern Pacific Ocean Areas

Takayabu (2002) noted that convective/stratiform rain over the ocean has almost synchronous diurnal variation with an early-morning maximum at 03–06 LST. Semidiurnal variation was reported for a NICAM aqua-planet simulation with a predawn peak at 03–06 LST and an afternoon peak at 12–15 LST (Tomita et al. 2005; Yasunaga et al. 2013). Yang and Smith (2008) noted that oceanic rainfall found at the global scale within the multiyear framework becomes very strong selectively at the seasonal-regional scale and depends on the year. Here, we studied semidiurnal variation in rainfall using the NICAM simulation over the eastern Pacific Ocean areas. Semidiurnal variation in rainfall over the ocean area is not seen clearly in the NICAM simulation (Fig. 2c). We select three oceanic areas: area I (150°–135°W, Eq.–10°N) and area II (135°–120°W, Eq.–10°N) cover the ITCZ and area III (180°–165°W, Eq.–10°S) is a relatively less convective area between the ITCZ and SPCZ.

Figure S1 shows the day-to-day variation in rainfall rate in the NICAM simulation (red) and GSMaP (purple) over area I (150°–135°W, Eq.–10°N) in UTC on 26–31 December 2006. NICAM does not show clear two peaks per day in contrast to our results for southern Africa and the Amazon. However, GSMaP shows two local peaks in a day on 27, 28, and 29 December. Although larger differences in rainfall rate between NICAM and GSMaP are seen on 26, 30, and 31 December, the rainfall rate shows reasonable agreement between NICAM and GSMaP on 27–29 December. Figure

S2a shows the mean daily variation in the rainfall observed by PR (blue), TMI (green) from the TRMM observation and GSMaP (purple: left ordinate) and the mean daily variation in the NICAM simulation (red; right ordinate) . NICAM and GSMaP indicate similar rainfall rate as a mean of about 0.4 mm hr^{-1}. Although the semidiurnal variation in rainfall rate is not seen in TMI and in NICAM, GSMaP shows semidiurnal variation with a primary peak in the early morning and a secondary peak in the evening around 19.5 LST. The early morning peak, around 6 LST, is seen in all data set. TMI and NICAM have one peak in the early morning at 5.5 LST. PR has a primary peak at 5.5 LST and a small peak at 12.5 LST. One peak per day in the early morning is the typical diurnal variation over the ocean area. The timing of the early morning peak is realistically captured by the NICAM simulation over this ocean area, although rainfall rate is higher than in TRMM TMI and PR.

Figure S2b shows the daily variation in convective (blue) and stratiform (green) rains in the PR observation in solid lines (left ordinate) and simulated convective (blue) and stratiform (green) rains by NICAM in dotted line (right ordinate) over area I (150°–135°W, Eq.–10°N). Here, convective rain in the NICAM simulation is defined as a rainfall rate higher than 10 mm hr^{-1}, and stratiform rain is defined as a rainfall rate lower than 5 mm hr^{-1}, which is the same method used in Fig. 7c and 10c. Stratiform rain in the PR observation has a higher rainfall rate than convective rain almost all day long, with a semidiurnal variation. The secondary peak of stratiform rainfall rate (at around 12 LST) in PR corresponds to the small peak of total rainfall rate in PR in Fig. S2a. Similar to the PR observation, the NICAM simulation of convective rain indicates an early-morning peak at the same time, at around 5.5 LST. The NICAM simulation of stratiform rain shows a gradual afternoon peak, although the amplitude of the diurnal variation is small. Whether the secondary peak of stratiform rainfall rate in PR and this tiny and gradual afternoon peak in NICAM is related or not is of interest, although the timing of the peaks is 3-6 hours apart. Although rainfall rate is higher than in PR/TMI, the NICAM simulation represents the early morning peak well. The semidiurnal peak is not clearly simulated by NICAM, probably because the stratiform rain is not well represented over this area of the ocean. This result may depend on the method used to classify convective and stratiform rain types. Further analysis of the characteristics of stratiform rains in NICAM are required to understand the difference from the observation.

Figure S3 shows the day-to-day variation in rainfall rate in NICAM (red) and GSMaP (purple) over area II (135°–120°W, Eq.–10°N) in UTC on 26–31 December 2006. GSMaP shows two peaks in a day on 28, 29 and 31 December, but they are not seen in the NICAM simulation. The higher rainfall rate at 00 UTC (15.5 LST) on the first and last day in both NICAM and GSMaP is remarkable, as it suggests abnormal rainfall conditions over this area. In contrast to Fig. S1, GSMaP indicates a higher rainfall rate on 27–30 December over this area.

Figure S4a shows the mean daily variation in rainfall rate in PR (blue), TMI (green), GSMaP (purple), and NICAM (red) over area II (135°–120°W, Eq.–10°N) (ordinate for TRMM and NICAM is the same in this case). The mean rainfall rate in the NICAM simulation is between those found in PR and TMI, with the primary peak in the early morning at 02 LST and a small secondary peak in the afternoon at 15.5 LST. As a mean rainfall rate during the six days, the peaks at 00 UTC on 26, 31 correspond to the peak at 15.5 LST and the peaks at ~12 UTC on 27, 29 and 30 corresponds to ~2 LST. The semidiurnal variation, with a primary peak from midnight to early in the morning and a secondary peak at 15.5 LST, is seen in PR and TMI. Note that PR shows a small minimum at 03 LST, so the daily variation in PR seems to have three peaks in a day. The NICAM simulation shows similar semidiurnal variation to TMI and PR, although the timing of the peaks is slightly different between NICAM and TRMM. GSMaP shows a primary peak at 6.5–8.5 LST and secondary peak at 14.5 LST. Although day-to-day variation in NICAM does not show any two peaks in a day, the mean value of rainfall rate NICAM over this area indicates semidiurnal variation, consistent with TRMM observations over this ocean area.

Convective (blue) and stratiform (green) rain in the PR observation (solid line) and the NICAM simulation (dotted line) over area II (135°–120°W, Eq.–10°N) are shown in Fig. S4b. The classification of convective and stratiform rains by NICAM is the same as in Figs. 7c, 10c, and S2b. Convective rainfall rate in PR is slightly higher than stratiform rainfall rate in PR from late afternoon to early morning over this area. The three peaks per day of total rain in PR (Fig. S4a) corresponding to two peaks of convective and stratiform rainfall rates between midnight and the early morning, and to the afternoon peak of stratiform rainfall rate. Although variation in convective/stratiform rain is generally synchronized, as noted by Takayabu (2002), the small peak of stratiform rain in the afternoon at 15 LST over this area is not seen for convective rain. Convective rainfall rate in the NICAM simulation shows peaks from midnight to early morning, again consistent with convective rainfall rate in the PR observation, although the timing of the earlier peak is different (2 LST). Stratiform rainfall rate in the NICAM simulation is lower than in PR, and shows two peaks in a day. Although the rainfall rate of stratiform rain in NICAM is smaller than convective rain in NICAM, as is similar to the other areas, the NICAM stratiform rainfall shows the semidiurnal variation with afternoon peak at 15.5 LST, consistent with the PR stratiform rainfall.

We also examined the semidiurnal variation over area III (180°–165°W, Eq.–10°S), where the semidiurnal variation is clearly seen for both TRMM and NICAM as shown by Figs. 2a, c, respectively. This area is between the ITCZ and the SPCZ, and rainfall rate over this area is relatively lower in the TRMM observation and the NICAM simulation compared to areas I and II (Fig. 1). The day-to-day variation in rainfall in NICAM (red) and GSMaP (purple) over this area is shown in Fig. S5 in UTC on 26–31 December 2006. Two peaks per day are clearly seen on the first day, followed by quasi-duo peaks per day on a couple of days in both NICAM and GSMaP with almost comparable rainfall rates. The time series of NICAM rainfall on the first day is similar to that of GSMaP for both rainfall rates and the timing of local peaks; the intensity of rainfall rate is relatively lower in NICAM than in GSMaP, and the peak is about 1–2 hours later in NICAM than in GSMaP. Figure S6a shows the mean daily variation in rainfall rate by PR (blue), TMI (green), and GSMaP (purple), whose values are shown on the left ordinate, by comparing with NICAM (red: right ordinate) over this area. Both TRMM and NICAM show the semidiurnal variation in rainfall rate, although the magnitude of rainfall rate is about ten times larger in TRMM. NICAM shows the primary peak in the morning at 8 LST with a small minimum at 6.5 LST and a secondary peak in the afternoon at 17 LST. PR (TMI) also indicates the primary peak in the morning at 4.5 LST and a secondary peak in the afternoon at 17.5 LST. GSMaP shows semidiurnal variation with a primary peak at 5.5 LST and a slightly earlier secondary peak at 13.5 LST. The rainfall rate is similar between NICAM and GSMaP over this area (note that the ordinates are different between GSMaP and NICAM). Here the primary peak in the NICAM simulation appears 3 hours later than in PR/TMI. We speculate that the difference in the magnitude of the rainfall rate between NICAM and TRMM may be due to the difference in the time for the analysis; if the one-week period is specified, the observation and the simulation are almost comparable, as revealed by the comparison between NICAM and GSMaP (Fig. S5).

Figure S6b shows the daily variation in convective (blue) and stratiform (green) rainfall rates in the PR observation (solid line) and the NICAM simulation (dotted line). The dual peak of total rain in PR coincides with the peak of both convective and stratiform rain. In PR, variation in convective and stratiform rainfall rate is almost synchronized over this area, whereas in NICAM, the semidiurnal peak of total rainfall rate is mostly by convective rain. Convective rainfall rate in NICAM indicates a dual peak, however, stratiform rainfall rate shows only a morning peak over this area. It is interesting that the small peak of total rainfall rate at 5 LST in NICAM corresponds to the peak of stratiform rainfall rate in the NICAM simulation. NICAM semidiurnal variation is caused mostly by convective rain as seen over the eastern Pacific Ocean areas in this study (Figs. S2b, S4b). In this area only, the stratiform rainfall rate has a morning peak, and there is no afternoon peak of stratiform rainfall rate.

The NICAM simulation shows a diurnal variation in rainfall rate as a mean value over the selected areas over the eastern Pacific Ocean. In the areas where the observation shows semidiurnal variation, the NICAM simulations show the semidiurnal variation on average. In general, however, the characteristics of stratiform rain are slightly different for these areas. The contrast between convective and stratiform rainfall rate is much stronger in the NICAM simulation than in the observation.

In the NICAM simulation, although the convective rain is stronger, the stratiform rain also contributes to the peaks. The difference between the observation and the simulation may also come from the difference in the analysis period: TRMM uses 17-year climatology where NICAM is a one-week simulation. Yang and Smith (2008) noted that the relatively weak afternoon secondary peak of oceanic rainfall found at the global scale within the multiyear framework becomes very strong selectively at the seasonal–regional scale.

S.2 Maritime Continent

The coastal region is affected by land-sea breezes caused by diurnally varying thermal contrast of water and dry land. A convective storm associated with the land-sea breeze propagate. Thus, the maritime continent area is known to have the complex feature of diurnal variation in rainfall rate (e.g., Mori et al. 2004: Sato et al. 2009). We studied the semidiurnal variation in rainfall over maritime continent areas N (120°–135°E, Eq.–10°N) and S (120°–135°E, Eq.–10°S). These areas are mixture of islands and ocean between Kalimantan and New Guinea islands, and they are thought to be representative of the complex nature of the maritime continent areas. The semidiurnal variation in rainfall can be seen in the observation and the simulation (Figs. 1a, c).

Figure S7 shows day-to-day variation of rainfall rate in NICAM (red) and GSMaP (purple) over area N (120°–135°E, Eq.–10°N). NICAM shows two peaks in a day on 26, 27, 28 and 29, while GSMap shows two peaks in a day on 27, 28, 29 and 30. Rainfall rate is similar on 30 and 31, although large difference between NICAM and GSMaP on first two days.

Figure S8a shows daily variation in rainfall rate in PR (blue), TMI (green), GSMaP (purple), and NICAM (red) over area N (120°–135°E, Eq.–10°N). The corresponding semidiurnal variation in convective (blue) and stratiform (green) rainfall rates in PR (solid line) and NICAM (dotted line) is shown in Fig. S8b. Note that the ordinate is different between TRMM and NICAM. In Fig. S8a, NICAM and TMI indicate semidiurnal variation via a primary peak in the morning and a secondary peak in the afternoon, while PR indicates three peaks in a day. We note that rainfall rate in NICAM is closer to that shown in GSMaP than to those shown in PR and TMI.

The NICAM simulation shows a primary peak at 4–7 LST and a secondary peak at 16 LST. The TMI shows semidiurnal variation with a primary peak at 3.5 LST and a secondary peak at 15.5 LST. The PR observation shows a primary peak at a similar time, 4.5 LST, and a secondary peak at 18.5 LST in the afternoon. GSMaP does not show semidiurnal variation over this area. Diurnal variation in convective and stratiform rainfall rates is generally synchronized over this maritime continent area, except around the peak at 18.5 LST. The peak of total rainfall rate at 18.5 LST in the PR observation coincides with the peak of stratiform rain in PR. Variation in convective rainfall rate is similar in the NICAM simulation and the PR observation, although the two peaks are slightly later in NICAM than in PR. The afternoon peak of convective rainfall rate in the NICAM simulation is at 15.5 LST. Stratiform rainfall rate in NICAM shows a morning peak at 6 LST; it is notable that the amplitude of the rainfall rate in NICAM is similar to that of the stratiform rainfall rate in PR (note each ordinate), while the convective rainfall rate in NICAM is lower than in PR.

For the southern hemispheric area S (120°–135°E, Eq.–10°S), the day-to-day variation for NICAM (red) and GSMaP (purple) are shown in Fig. S9. NICAM shows two peaks in a day on 30 and 31, while GSMaP shows two peaks in a day on 28, 29 and 31. The daily variation in rainfall (Fig. S10a), and in convective and stratiform rainfall rates (Fig. S10b) is similar to that found in the northern hemispheric area N (120°–135°E, Eq.–10°N) (Figs. S8a, b). Again, we can see the semidiurnal variation in rainfall rate in NICAM, PR, and TMI with an early morning peak and an afternoon peak. However, GSMaP does not show semidiurnal variation in rainfall rate. Mixture of the surface properties of land and ocean might affect rainfall rate estimation by the microwave and infrared data used for the GSMaP retrieval. Even though two peaks in a day are seen in the day-to-day variation, slight lag of the peak time might shift the peak computed as six days mean. Timing of the primary peak in the early morning at 3.5 LST and a secondary peak in the afternoon at ~15 LST is close to both PR/TMI and NICAM, although the rainfall rate in the NICAM simulation is almost twice as high as in the observations. Convective/stratiform rainfall rate in PR (blue/green: solid line in Fig. S10b) varies in a synchronized manner over this area S as well, although convective rainfall rate is higher than stratiform rainfall rate. In the NICAM simulation, the semidiurnal variation in convective rainfall rate is greater than that of stratiform rainfall rate (as seen in Fig. S8b), although the timing of the peak of convective rainfall rate is close to that seen the PR observation.

The details of the daily variations are different for the two adjacent areas N and S. However, the semidiurnal variation shows a primary peak in the early morning and a secondary peak in the afternoon peak in both areas. It is interesting that although the total rainfall rate in PR is almost the same between the two areas (0.2–0.3 mm hr^{-1}), the contribution of convective rainfall rate is larger over area S than over area N. The contrast of land/sea areal size between N and S might be one reason for this difference; convective rain may be more active as the land area increases.

References

Takayabu, Y. N., 2002: Spectral representation of rain profiles and diurnal variations observed with TRMM PR over the equatorial area. *Geophys. Res. Lett.*, **29**, 1584, doi:10.1029/2001GL014113.

Tomita, H., H. Miura, S. Iga, T. Nasuno, and M. Satoh, 2005: A global cloud-resolving simulation: Preliminary results from an aqua planet experiment. *Geophys. Res. Lett.*, **32**, L08805, doi:10.1029/2005GL022459.

Yang, S., and E. A. Smith, 2008, Convective-stratiform precipitation variability at seasonal scale from 8 yr of TRMM observations: Implications for multiple modes of diurnal variability. *J. Climate*, **21**, 4087–4114.

Yasunaga, K., T. Nasuno, H. Miura, Y. N. Takayabu, and M. Yoshizaki, 2013: Afternoon precipitation peak in an aqua-planet global non-hydrostatic model (Aqua-planet NICAM). *J. Meteor. Soc. Japan,* **91A**, 217-229.

Figure

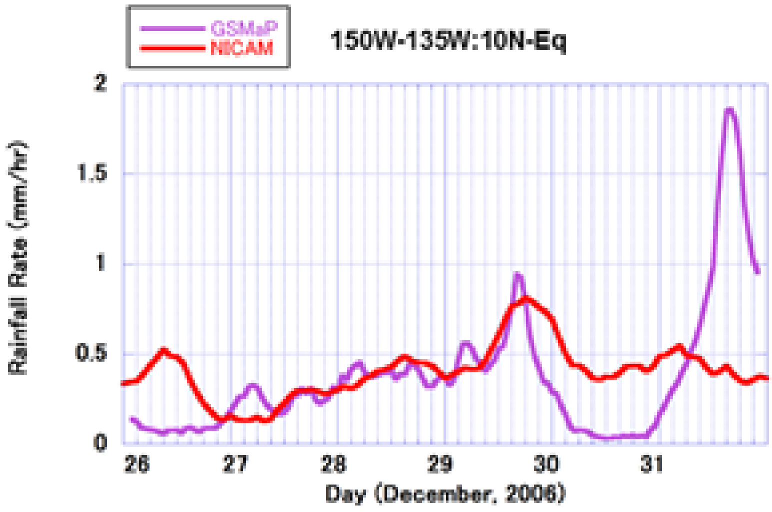

Figure S1:

Same as Fig. 3 but for eastern Pacific Ocean area I (150°-135°W, Eq.-10°N). The *x*-axis starting at 14.5 LST on 26 December 2006.

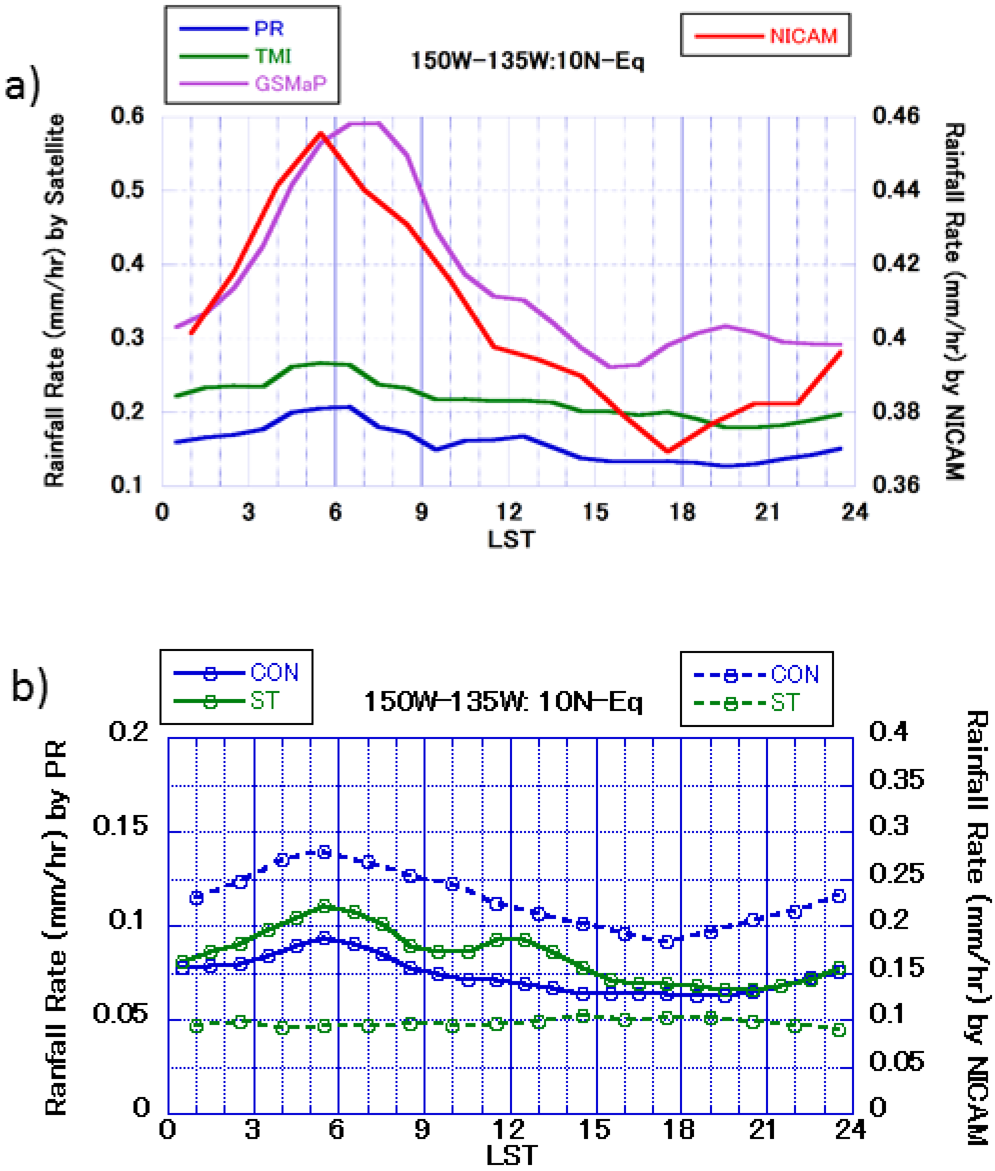

Figure S2:
(a) and (b) Same as Fig. 4 and Fig. 7c, respectively, but for eastern Pacific Ocean area I (150°-135°W, Eq.-10°N).

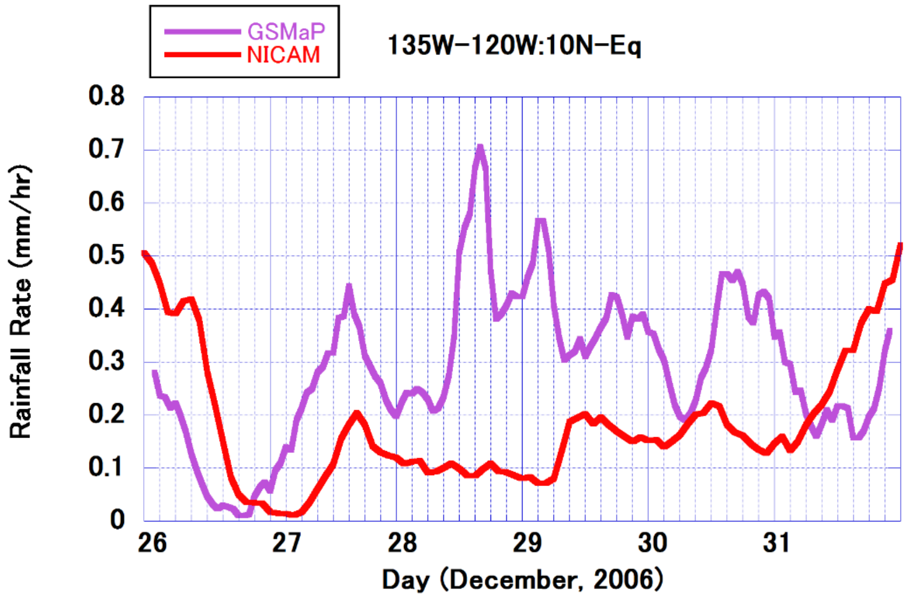

Figure S3:

Same as Fig. 3 but for eastern Pacific Ocean area II (135°-120°W, Eq.-10°N-Eq.). The *x*-axis starting at 15.5 LST on 26 December 2006.

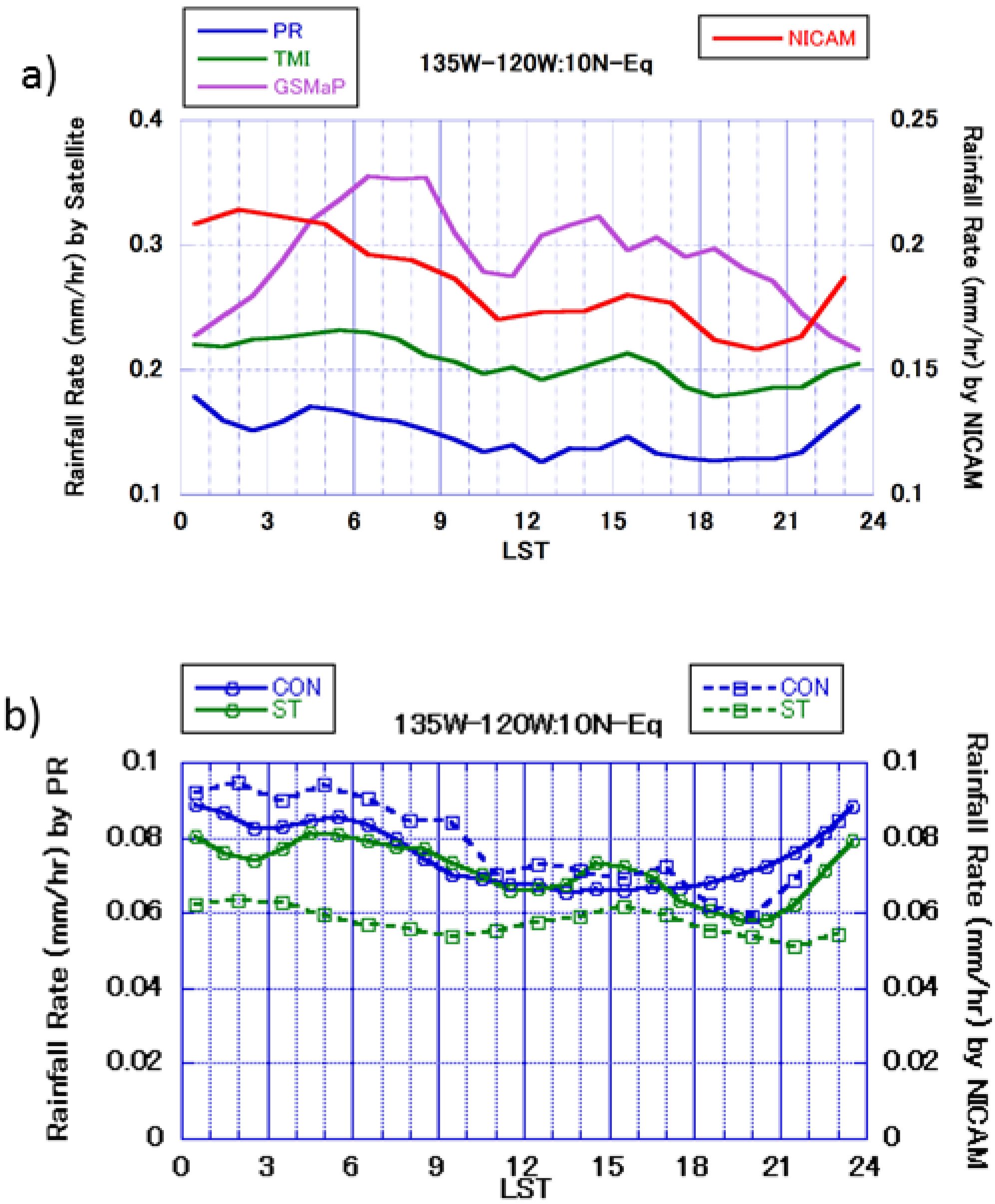

Figure S4:

(a) and (b) Same as Fig. 4 and Fig. 7c, respectively, but for eastern Pacific Ocean area II (135°-120°W, Eq.-10°N).

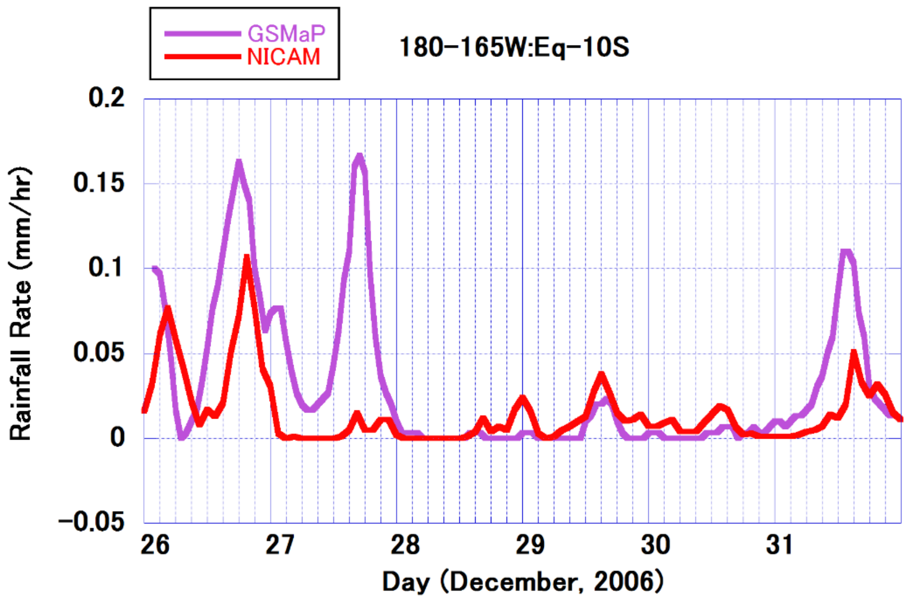

FigureS5:

Same as Fig. 3 but for eastern Pacific Ocean area III (180°-165°W, Eq.-10°S). The *x*-axis starting at 12.5 LST on 26 December 2006.

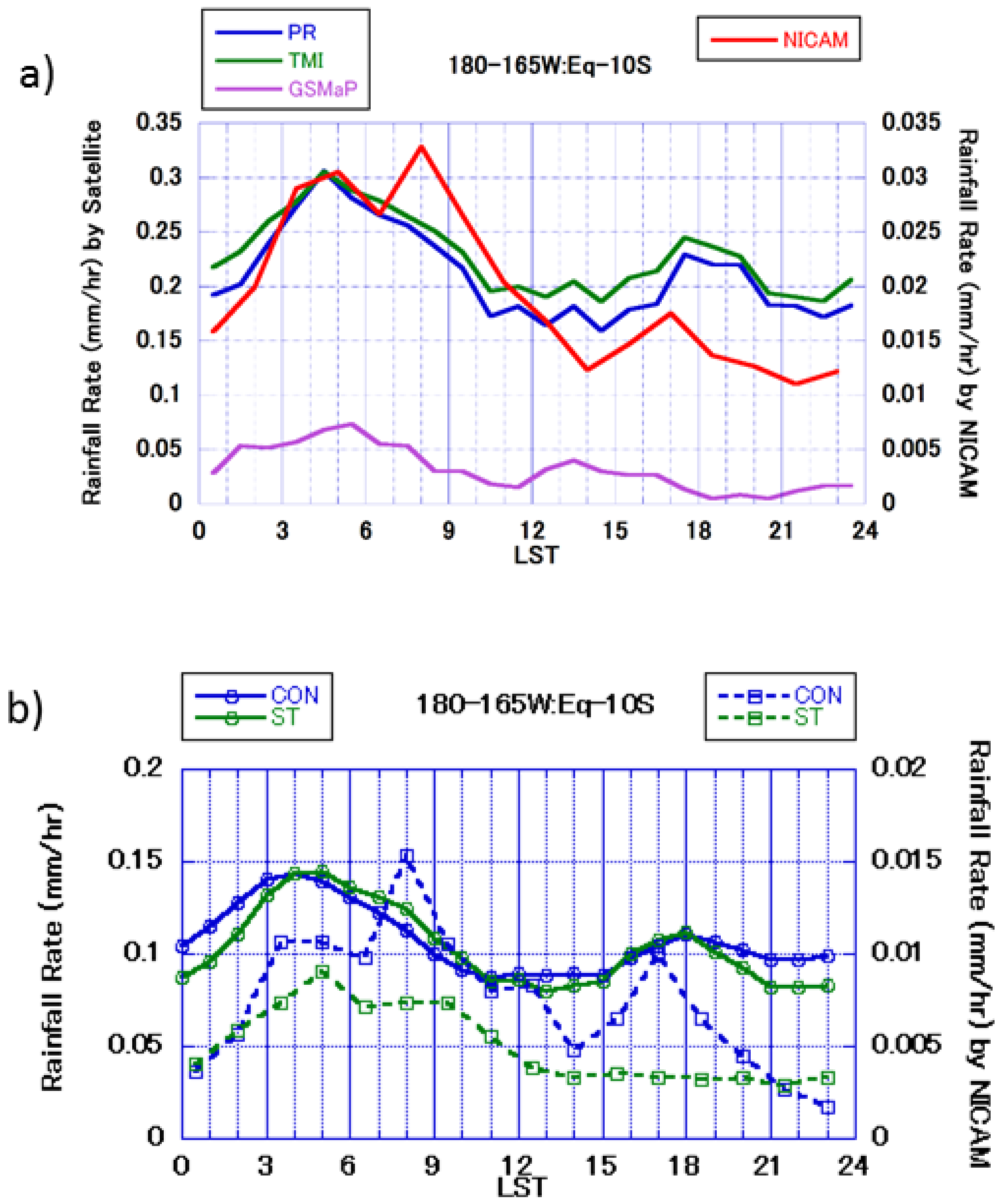

Figure S6:

(a) and (b) Same as Fig. 4 and Fig. 7c, respectively, but for eastern Pacific Ocean area III (180°-165°W, and Eq.-10°S).

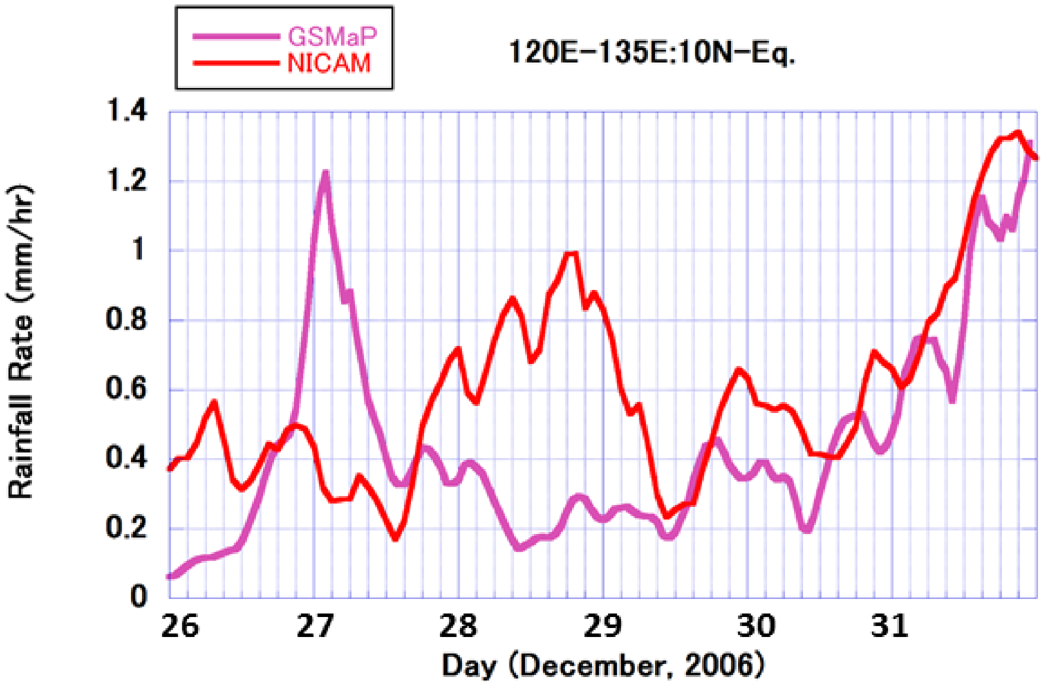

Figure S7:

Same as Fig. 3 but for maritime continent area N (120°-135°E, Eq.-10°N). The *x*-axis starting at 8.5 LST on 26 December 2006.

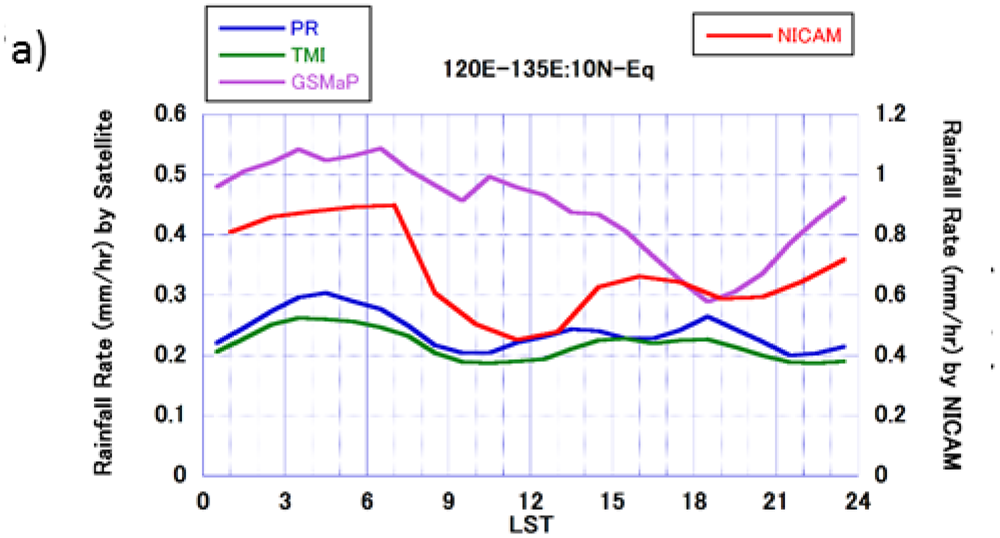

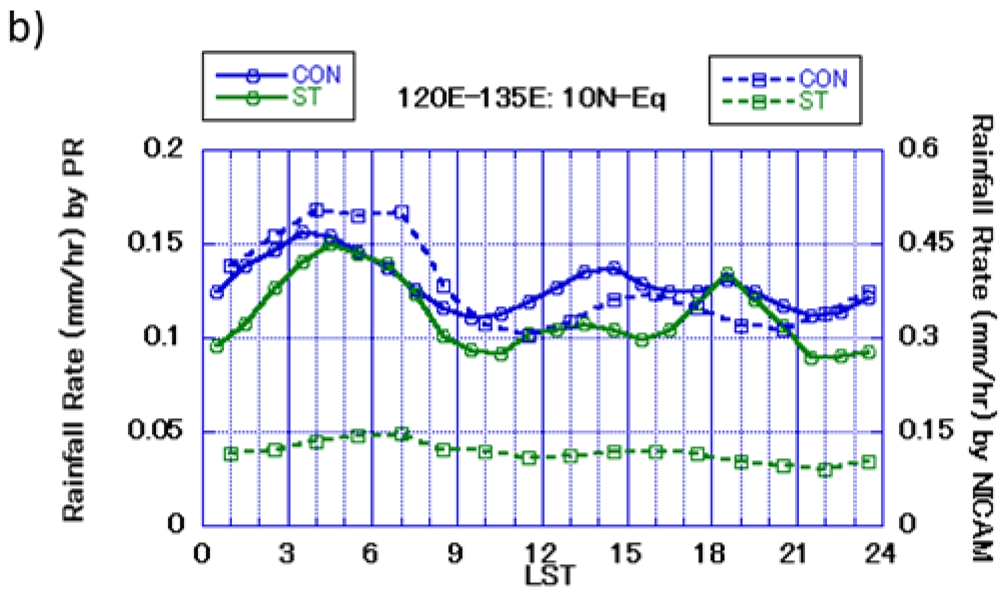

Figure S8:

(a) and (b) Same as Fig. 4 and Fig. 7c, respectively, but for the maritime continent area N

(120°-135°E, Eq.-10°N).

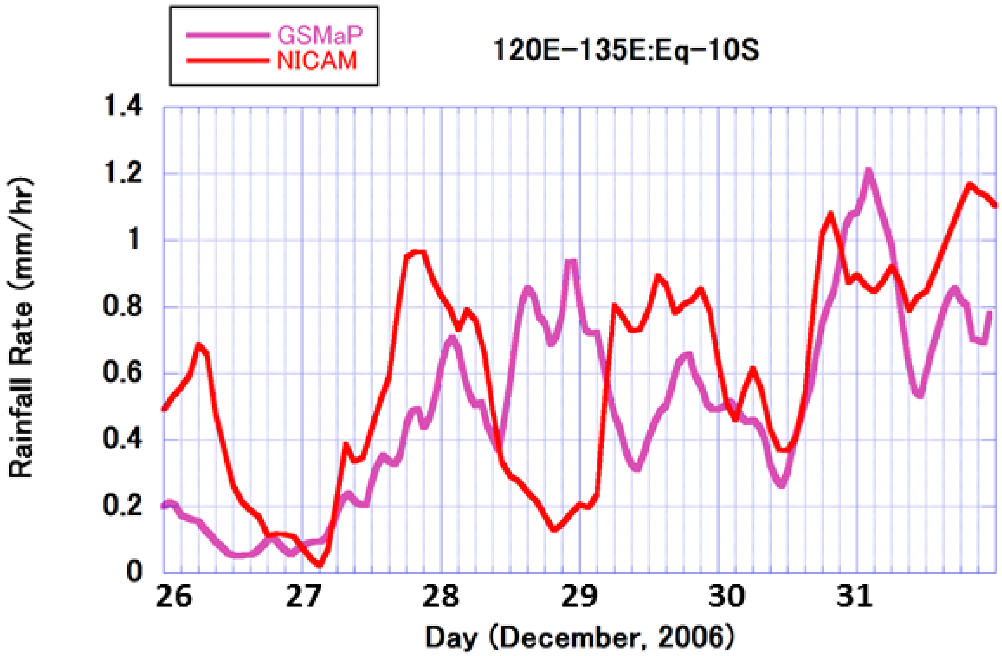

Figure S9:

Same as Fig.3 but for maritime continent area S (120°-135°E, Eq.-10°S). The *x*-axis starting at 8.5 LST on 26 December 2006.

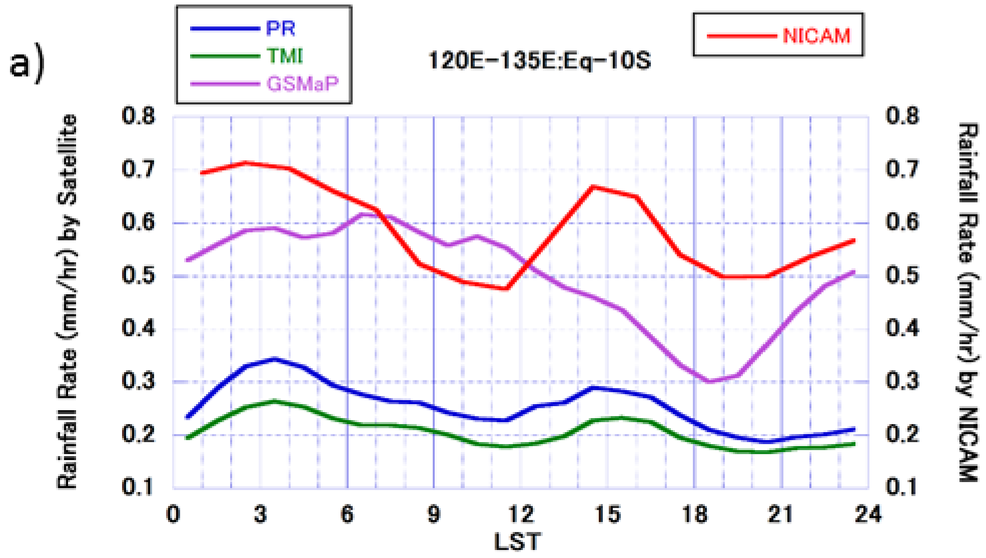

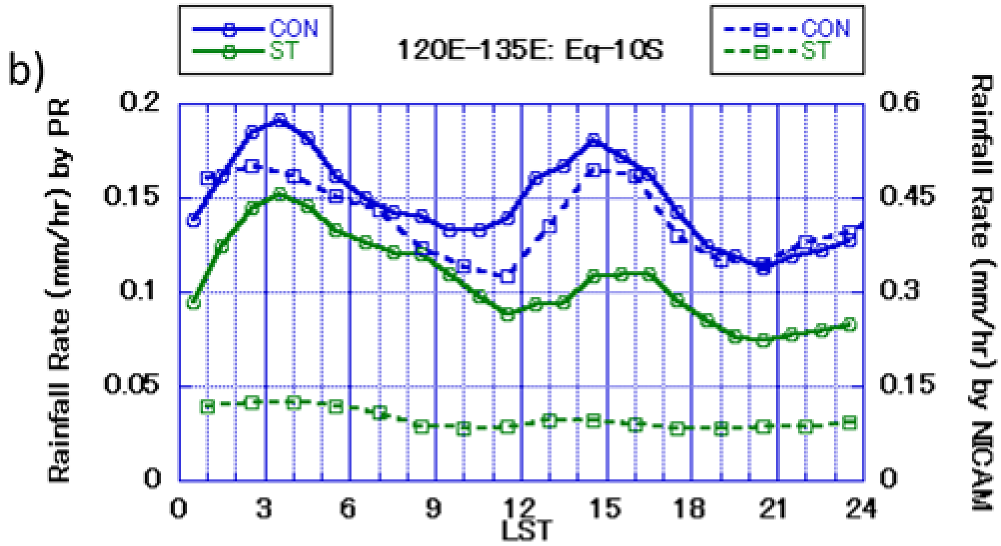

Figure S10:
(a) and (b) Same as Fig. 4 and Fig. 7c, respectively, but for the maritime continent area S (120°-135°E, Eq.-10°S).